Research Square

Preprints are preliminary reports that have not undergone peer review.
They should not be considered conclusive, used to inform clinical practice,
or referenced by the media as validated information.

Development and internal validation of an ordinal risk-stratification model for respiratory–renal deterioration after postoperative acute kidney injury in acute type A aortic dissection: a retrospective cohort study

Xiaoran Shen
Capital Medical University, Beijing Institute of Heart, Lung and Blood Vessel Diseases
Runqiao Li
Beijing Anzhen Hospital
Jianji Wang
Beijing Anzhen Hospital
Jiazhen Mei
Beijing Anzhen Hospital
Peiyuan Yao
Beijing Anzhen Hospital
Tingxuan Yan
Beijing Anzhen Hospital
Ningning Liu
Shanxi Cardiovascular Hospital, Shanxi Medical University
Jinhui Ma
Zhengzhou University School of Medicine
Biren Zheng
Beijing Anzhen Hospital
Baoshu Chen
Beijing Anzhen Hospital
Chengnan Li
Beijing Anzhen Hospital
Yipeng Ge
yipengge@126.com

Capital Medical University, Beijing Institute of Heart, Lung and Blood Vessel Diseases
Junming Zhu

Capital Medical University, Beijing Institute of Heart, Lung and Blood Vessel Diseases

Research Article

Keywords: acute kidney injury, acute type A aortic dissection, respiratory failure, continuous renal replacement therapy, ordinal prediction, internal validation

Posted Date: November 25th, 2026

DOI: https://doi.org/10.21203/rs.3.rs-11442029/v1

License: This work is licensed under a Creative Commons Attribution 4.0 International License. Read Full License

Additional Declarations: No competing interests reported.

Development and internal validation of an ordinal risk-stratification model for respiratory–renal deterioration after postoperative acute kidney injury in acute type A aortic dissection: a retrospective cohort study

Research article

Xiaoran Shen[a], Runqiao Li[a], Jianji Wang[a], Jiazhen Mei[a], Peiyuan Yao[a], Tingxuan Yan[a], Ningning Liu[b], Jinhui Ma[c], Biren Zheng[a], Baoshu Chen[a], Chengnan Li[a], Yipeng Ge[a], Junming Zhu[a]

[a] Department of Cardiovascular Surgery, Beijing Anzhen Hospital, Capital Medical University; Beijing Aortic Disease Center; Beijing Institute of Heart, Lung and Blood Vessel Diseases, No. 2 Anzhen Road, Chaoyang District, Beijing 100029, China.

[b] Department of Cardiovascular Surgery, Shanxi Cardiovascular Hospital, Shanxi Medical University, No. 18 Yifen Street, Taiyuan 030024, Shanxi, China.

[c] Department of Vascular Surgery, Henan Provincial People's Hospital, Zhengzhou University School of Medicine, No. 7 Weiwu Road, Jinshui District, Zhengzhou 450003, Henan, China.

Corresponding author: Yipeng Ge, MD, Beijing Anzhen Hospital, Capital Medical University, No. 2 Anzhen Road, Chaoyang District, Beijing 100029, China. Email: yipengge@mail.ccmu.edu.cn.

Abstract

Background: Respiratory failure after acute kidney injury (AKI) following acute type A aortic dissection repair may occur without continuous renal replacement therapy (CRRT). We examined whether it identifies an intermediate-risk state and developed an ordinal risk-stratification framework at AKI onset.

Methods: This retrospective analysis included 601 patients with postoperative AKI. First fulfillment of AKI criteria defined the index time. Outcomes were Grade 0 (neither respiratory failure nor CRRT), Grade 1 (respiratory failure without CRRT), and Grade 2 (CRRT irrespective of respiratory status). Regularized ordinal logistic regression was evaluated using repeated nested cross-validation

and comparison with three ensemble models. Ranked probability score (RPS) was the primary metric.

Results: Grades 0, 1, and 2 included 285 (47.4%), 170 (28.3%), and 146 (24.3%) patients. In-hospital mortality was 1.1%, 10.6%, and 25.3%; median intensive care unit stay was 57, 192, and 204 h. The ordinal model achieved RPS 0.1705 and areas under the receiver operating characteristic curve of 0.7476 for Grade ≥1 and 0.8299 for Grade 2. Inflammatory features lowered RPS by 0.0109 (95% confidence interval, 0.0042-0.0182) versus the non-inflammatory model. Glucose-to-albumin ratio and immediate respiratory measurements added little.

Conclusions: Respiratory failure without CRRT identified an intermediate-risk post-AKI state. The ordinal model provided an exploratory framework for subsequent respiratory–renal deterioration, with strongest discrimination at the CRRT threshold.

Trial registration: Parent cohort: Chinese Clinical Trial Registry, ChiCTR2500112924, retrospectively registered on 21 November 2025. The present study is an observational secondary analysis.

Keywords: acute kidney injury; acute type A aortic dissection; respiratory failure; continuous renal replacement therapy; ordinal prediction; internal validation

Background

Acute kidney injury (AKI) is common after surgical repair for acute type A aortic dissection (ATAAD) and is associated with adverse outcomes [1-4]. Most prediction studies focus on incident or severe AKI [2,5-7]. Once AKI develops, patients may experience respiratory failure without requiring continuous renal replacement therapy (CRRT).

Using CRRT alone as the endpoint would group these intermediate-risk patients together with those who experience neither event. We therefore examined three ordered post-AKI states: neither event, respiratory failure without CRRT, and subsequent CRRT irrespective of respiratory status.

Blood-cell-derived inflammatory indices and albumin-related markers have been associated with AKI after aortic and cardiac surgery [8-13]; the glucose-to-albumin ratio (GAR) has been linked to outcomes in critically ill cardiovascular patients [14]. Whether these markers improve prediction after AKI onset is unclear.

In this study, we characterized the clinical severity gradient across three ordered post-AKI respiratory–renal states. Using the first postoperative fulfillment of KDIGO AKI criteria as the index time, we then developed and internally validated an ordinal risk-stratification framework [15]. We compared regularized ordinal regression with ensemble models and examined the incremental value of inflammatory features, GAR, and direct respiratory measurements. We further considered the potential implications of this framework for post-AKI monitoring and critical-care resource allocation.

Methods

Study design and population

This single-center retrospective cohort study was a secondary analysis of prospectively collected data from an institutional cohort at Beijing Anzhen Hospital, Capital Medical University, a tertiary cardiovascular center in China. The parent cohort was retrospectively registered with the Chinese Clinical Trial Registry (ChiCTR2500112924) on 21 November 2025. The database used for the present analysis was locked on July 30, 2026.

Participants in the parent cohort who underwent ATAAD repair between April 18, 2024, and June 30, 2026 and developed postoperative AKI according to Kidney Disease: Improving Global Outcomes (KDIGO) criteria were screened for the present analysis. Eligibility criteria for the parent cohort are provided in Supplementary Methods S2 (Additional file 1). AKI was diagnosed using serum creatinine or urine output criteria; baseline serum creatinine was the most recent preoperative measurement. The patient-specific index time was defined as the first postoperative fulfillment of KDIGO AKI criteria. To be included, patients had to meet all of the following criteria before the

index time: alive; no mechanical ventilation for >48 h; no reintubation; and no initiation of continuous renal replacement therapy (CRRT). The sample size was determined by the number of eligible patients during the study period; no formal sample-size calculation was performed. The parent cohort comprised 1186 patients; 579 did not develop postoperative AKI. Among the 607 patients with postoperative AKI, six were excluded for mutually exclusive events before the index time: CRRT initiation (n = 3), reintubation (n = 2), or death (n = 1). The final analysis included 601 patients. This study was reported in accordance with the TRIPOD+AI statement [16].

The study was conducted in accordance with the Declaration of Helsinki and its subsequent amendments. The parent cohort and secondary use of its data were approved by the Ethics Committee of Beijing Anzhen Hospital (approval No. KS2024036; April 17, 2024). Written informed consent was obtained from all participants at enrollment. The present analysis was separately approved by the same committee (approval No. 2026311x; September 7, 2026), which waived the requirement for additional informed consent.

Data collection and candidate predictors

Candidate predictors were extracted from the electronic medical record and restricted to routinely available measurements obtained before the index time. They included demographic and anthropometric characteristics, medical history, preoperative laboratory variables, intraoperative variables, and immediate postoperative laboratory measurements. Preoperative variables were the most recent values before surgery. Intraoperative variables included blood-product transfusion, estimated blood loss, fluid input and output, urine output, total operative time, cardiopulmonary bypass (CPB) duration, and aortic cross-clamp time. Immediate postoperative variables were the first measurements within 2 h after surgery and preceded the index time in all included patients.

Derived candidate predictors were neutrophil-to-lymphocyte ratio (NLR), platelet-to-lymphocyte ratio (PLR), monocyte-to-lymphocyte ratio (MLR), neutrophil-to-platelet ratio (NPR), systemic immune-inflammation index (SII), systemic inflammation response index (SIRI), aggregate index

of systemic inflammation (AISI), and glucose-to-albumin ratio (GAR). They were calculated from observed source measurements before fitting. The cell-count indices were natural log-transformed; GAR was glucose/albumin without log transformation. Missingness was ≤5% for each candidate and was handled within training folds. Definitions, units, windows, and missingness are in Supplementary Tables S1–S2. Post-index measurements and outcomes were not used as predictors.

Surgical procedures

All procedures were performed through median sternotomy using CPB. Anesthetic, cannulation, cerebral-perfusion, and reconstruction strategies were individualized according to dissection anatomy and operative requirements. Arch procedures used unilateral or bilateral antegrade selective cerebral perfusion under moderate hypothermic circulatory arrest (26–28°C). Hemiarch, island arch, total arch, and aortic-root procedures were performed as clinically indicated. Detailed operative techniques are provided in Supplementary Methods S1.

Outcome definition

Follow-up began at the index time and ended at hospital discharge or in-hospital death. Grade 0 indicated neither respiratory failure nor CRRT after the index time; Grade 1 indicated respiratory failure without subsequent CRRT; and Grade 2 indicated CRRT initiation after the index time, irrespective of respiratory-failure status. For descriptive analyses of postoperative AKI severity, AKI stage was determined using KDIGO serum creatinine and urine-output criteria only; the renal replacement therapy (RRT) criterion was excluded because post-index CRRT defined Grade 2. Respiratory failure was defined as invasive mechanical ventilation >48 h, with the threshold first crossed after the index time, or reintubation after the index time. Grade 2 was further characterized as Grade 2a (CRRT without respiratory failure) and Grade 2b (CRRT with respiratory failure). Mortality was not incorporated into grading and was analyzed separately. Temporal eligibility and outcome classification were adjudicated from source timestamps before construction of the de-identified analytic dataset (Supplementary Methods S2 and Supplementary Table S3).

Model development and internal validation

The primary model was L2-regularized proportional-odds ordinal logistic regression; comparators were ordinal random forest, XGBoost, and LightGBM. Tree-based models estimated $P(Y \geq 1)$ and $P(Y \geq 2)$ separately, enforced monotonicity, and reconstructed grade probabilities. The expected score was calculated as $P(Y=1)+2P(Y=2)$. Boruta selected predictors [17]; Spearman correlations, variance inflation factors, and condition indices assessed collinearity. Shapley additive explanations (SHAP) summarized model contributions [18]. Internal validation used five outer folds repeated 10 times and five inner folds for tuning. Imputation, transformation, standardization, selection, and tuning were fitted within each outer training fold. Each patient's 10 held-out probability predictions were averaged, and models used identical outer folds.

The pipeline was refitted on all 601 patients for the research-use calculator. Reported performance uses averaged out-of-fold predictions. Calculator coefficients and ranges, model comparisons, and implementation details are in Supplementary Table S4, Tables S5–S6, and Supplementary Methods S3–S7.

Statistical analysis and model performance

Continuous variables were summarized as mean ± standard deviation or median (interquartile range), and categorical variables as n (%). Between-grade comparisons used parametric, nonparametric, χ^2, or exact tests as appropriate. Jonckheere–Terpstra and Cochran–Armitage tests assessed trends in expected scores and in-hospital mortality. The ranked probability score (RPS) was the primary metric; secondary metrics were normalized multiclass Brier score, ordinal C-index, areas under the receiver operating characteristic curve (AUCs) for Grade ≥1 and Grade 2, mean absolute error, and weighted kappa. Threshold-specific calibration used decile plots and patient-level intercepts, slopes, and observed-to-expected ratios [19]; decision curves assessed net benefit [20]. Patient-level bootstrap resampling of averaged out-of-fold predictions yielded 95% confidence

intervals and paired comparisons. Holm adjustment was used within model-comparison families; tests were two-sided with $P<0.05$.

Sensitivity and feature-set analyses

Sensitivity analyses examined Grade 2 subtypes, threshold-specific and multinomial models, a seven-variable model, complete-case and alternative-imputation analyses. Because death before fulfillment of the >48-h ventilation criterion could limit the opportunity for classification as respiratory failure, we repeated the analyses after excluding the three Grade 0 deaths and after reassigning them to Grade 2. Feature-set analyses compared inflammatory representations with a common non-inflammatory reference model, examined GAR and its components, and added arterial partial pressure of carbon dioxide ($PaCO_2$), arterial partial pressure of oxygen (PaO_2), alveolar–arterial oxygen gradient ($A–aDO_2$), and the ratio of PaO_2 to fraction of inspired oxygen (PaO_2/FiO_2). Paired bootstrap estimates and adjustment rules are described in Supplementary Methods S8; results appear in Supplementary Tables S7–S11.

Use of generative AI in manuscript preparation

During the preparation of this work, the authors used ChatGPT (OpenAI) to assist with English-language editing. The tool was not used to generate data or perform statistical analyses. After using it, the authors reviewed and edited the content as needed and take full responsibility for the content of the published article.

Results

Study cohort and clinical phenotypes

A total of 1186 patients were included in the parent cohort, of whom 607 developed postoperative AKI. As shown in Figure 1A, six patients were excluded due to pre-index events (CRRT, n=3; reintubation, n=2; death, n=1), leaving 601 patients for the final analysis. Among these, 285 (47.4%) were Grade 0, 170 (28.3%) Grade 1, and 146 (24.3%) Grade 2; Grade 2 comprised 37

patients with CRRT alone (Grade 2a) and 109 with CRRT and respiratory failure (Grade 2b) (Figure 1A–C). Preoperative renal reserve, operative burden, and immediate postoperative abnormalities differed across grades (Table 1). Out-of-fold expected ordinal scores increased across grades: median 0.517 (interquartile range [IQR], 0.326–0.756) in Grade 0, 0.692 (0.502–0.964) in Grade 1, and 1.196 (0.841–1.513) in Grade 2 ($P < 0.001$ for trend; Figure 1D).

Median mechanical ventilation was 17.0 h in Grade 0, 116.5 h in Grade 1, and 119.5 h in Grade 2; median intensive care unit (ICU) stay was 57.0, 192.0, and 204.0 h, respectively (Table 2). In-hospital deaths numbered 3/285 (1.1%), 18/170 (10.6%), and 37/146 (25.3%; $P < 0.001$ for trend). Mortality was 24.3% in Grade 2a and 25.7% in Grade 2b; Grade 2b had longer ventilation and ICU stay.

Feature selection and predictive associations

Full-cohort Boruta analysis selected 14 predictors; outer-fold selection frequencies are shown in Figure 2C and Supplementary Figures S1–S2. Immediate postoperative creatinine, NPR, operative time, and GAR were prominent in model associations and SHAP summaries (Figure 2A–B; Supplementary Figures S3–S4 and Table S4).

Internal validation and model comparison

The ordinal logistic model achieved an out-of-fold RPS of 0.1705, normalized multiclass Brier score of 0.1794, ordinal C-index of 0.7632, and AUCs of 0.7476 for Grade ≥1 and 0.8299 for Grade 2 (Figure 3A; Table 3; Supplementary Table S5). Its RPS was lower than LightGBM's (difference, −0.0160; 95% confidence interval (CI), −0.0247 to −0.0085; Holm-adjusted $P < 0.001$); differences versus random forest and XGBoost were smaller and not consistently significant after adjustment (Supplementary Table S6). Calibration slopes were 1.04 for Grade 2 and 0.79 for Grade ≥1 (Figure 3B); the latter indicates somewhat too-extreme predicted risks. Decision curves suggested positive net benefit over the displayed threshold range, with a more consistent pattern for Grade 2 (Figure 3C).

Incremental-value and sensitivity analyses

Adding the selected inflammatory feature set reduced RPS by 0.0109 (95% CI, 0.0042–0.0182; P = 0.002) versus the non-inflammatory reference model (Figure 4; Supplementary Table S8). Raw counts and composite indices produced similar changes. Adding GAR to the model without GAR changed RPS by −0.0012 (95% CI, −0.0040 to 0.0019; P = 0.460); glucose and albumin representations performed similarly (Supplementary Table S7). Forced inclusion of $PaCO_2$, PaO_2, A–aDO_2, and PaO_2/FiO_2 did not appreciably improve RPS (Supplementary Table S9).

Multinomial and threshold-specific models did not consistently improve performance; the seven-variable model increased RPS by 0.0038 relative to the fixed 14-variable model. Complete-case analysis (n=567) yielded RPS 0.1710 and Grade 2 AUC 0.8253. Excluding the three Grade 0 deaths or assigning them to Grade 2 yielded RPS 0.1677 and 0.1671, respectively (Supplementary Table S10). Selection frequencies and model diagnostics appear in Supplementary Figure S8 and Table S11.

Reduced model and research-use calculator

The seven-variable model included NPR, immediate postoperative creatinine, operative time, lactate, GAR, preoperative estimated glomerular filtration rate (eGFR), and preoperative myoglobin. Its out-of-fold RPS was 0.1749 versus 0.1712 for the fixed 14-predictor model (Supplementary Table S10). After refitting on all 601 patients, it was implemented as a web-based research-use calculator that returns probabilities for Grades 0, 1, and 2 and the expected ordinal score (Supplementary Figure S9; Additional file 2; coefficients in Table S4).

Discussion

This study evaluated deterioration after postoperative AKI in ATAAD rather than predicting AKI occurrence. Respiratory failure without CRRT formed an intermediate-risk state between patients with neither event and those who initiated CRRT. The ordinal risk-stratification framework successfully captured this structure. Additionally, the inclusion of inflammatory features improved

overall probabilistic accuracy. The findings support assessing post-AKI respiratory and renal deterioration across more than a single CRRT threshold.

Clinically, recognizing respiratory failure without CRRT as a distinct intermediate state may prevent these patients from being overlooked. This is particularly important when CRRT alone is used as the endpoint. Their mortality and critical-care utilization were comparable to those of Grade 2 patients. This suggests they may require closer respiratory monitoring, more cautious extubation assessment, and greater ICU resource preparedness. Thus, the potential value of this three-grade framework lies not only in predicting CRRT but also in stratifying overall post-AKI deterioration risk.

Previous ATAAD prediction studies have mainly addressed incident or severe AKI [2,5-7]. Here, prediction began after AKI was established and focused on the subsequent clinical course. The 170 patients with respiratory failure but no CRRT had greater mortality and critical-care use than Grade 0 patients; a CRRT-only endpoint would combine these groups and conceal that difference. Mortality increased across Grades 0, 1, and 2, supporting the clinical relevance of the ordered categories, even though mortality was not included in the grading definition. Kidney–lung crosstalk provides a plausible biological basis for the respiratory phenotype after AKI [21].

The selected predictors span several parts of the perioperative risk profile. Immediate postoperative creatinine and preoperative eGFR represent current renal dysfunction and baseline reserve; operative time reflects procedural burden; lactate and myoglobin capture perfusion or tissue stress; and GAR and NPR add metabolic and inflammatory information. Perioperative myoglobin has been associated with AKI after ATAAD repair [22], while renal function, procedure duration, and hypoperfusion markers have also been linked to adverse renal outcomes [2,6,23]. Together, the predictors suggest that deterioration after AKI is associated with renal, operative, perfusion, and inflammatory factors.

The inflammatory feature set provided the clearest incremental improvement in RPS, and similar changes were observed when inflammatory information was represented by blood-cell counts,

composite indices, or both. This consistency supports the predictive value of the broader inflammatory domain, rather than a unique advantage of any single index like NPR. NPR combines neutrophil and platelet information relevant to innate immune activation and platelet–leukocyte interactions [24-25]. However, NPR, PLR, SII, and AISI share components and therefore carry overlapping information. Cardiopulmonary bypass-related inflammation, endothelial injury, and kidney–lung pathways provide a plausible clinical context for this association [21,26-27].

GAR and early respiratory measurements contributed less unique information. Removing GAR produced little change in RPS, and glucose and albumin yielded similar performance, suggesting that their information overlapped with the broader perioperative profile. Early PaO_2, $PaCO_2$, A–aDO_2, and PaO_2/FiO_2 measurements are influenced by FiO_2, ventilator settings, and sampling conditions. In contrast, the respiratory outcome in this study reflected prolonged ventilation or reintubation later in the admission. A single early measurement may not capture evolving lung injury, fluid management, and subsequent ventilatory care. Time-updated respiratory variables may therefore be more informative for predicting the respiratory-only grade.

The proportional-odds model achieved the lowest RPS among the evaluated models. However, its differences from random forest and XGBoost were not consistently significant after multiplicity adjustment. The results show that added model complexity did not provide a consistent gain in this cohort. The ordinal model directly returns probabilities for all three grades and offers a compact structure for research-use implementation. Performance also differed by threshold: discrimination was stronger for CRRT-defined Grade 2 than for Grade ≥1, indicating that the intermediate respiratory-only state remains more difficult to predict. This pattern is consistent with the multiple patient, operative, and care-related determinants of prolonged ventilation after ATAAD surgery [28-29].

Strengths and limitations

The prediction index time was based on the first postoperative fulfillment of KDIGO AKI criteria. All candidate predictors were measured prior to outcome-defining events. Furthermore, repeated nested cross-validation confined preprocessing and feature selection to the training folds. Evaluation included probabilistic accuracy, discrimination, calibration, and decision curves. The reduced seven-variable model had a similar, slightly higher RPS than the 14-predictor model and provides a practical specification for further testing.

We defined a three-level outcome to represent post-AKI respiratory–renal deterioration in this analysis. Prolonged ventilation and CRRT initiation are clinically relevant events but may also reflect local practice, therefore the ordinal framework requires evaluation across centers. This single-center retrospective analysis had internal validation only; external validation is needed to assess transportability and calibration. Exact event intervals were not retained in the analytic dataset, precluding time-to-event analyses.

Conclusions

Among patients with postoperative AKI after ATAAD repair, respiratory failure without CRRT identified an intermediate-risk state with mortality and critical-care burden between Grade 0 and Grade 2. The three-grade ordinal model provided an exploratory risk-stratification framework for subsequent respiratory–renal deterioration, with the strongest discrimination at the CRRT threshold. Additionally, the inclusion of inflammatory features improved overall prediction. This framework may help inform post-AKI monitoring and critical-care resource planning.

List of abbreviations

A–aDO_2, alveolar–arterial oxygen gradient; AISI, aggregate index of systemic inflammation; AKI, acute kidney injury; ATAAD, acute type A aortic dissection; AUC, area under the receiver operating characteristic curve; CI, confidence interval; CPB, cardiopulmonary bypass; CRRT, continuous renal replacement therapy; eGFR, estimated glomerular filtration rate; GAR, glucose-to-

albumin ratio; ICU, intensive care unit; IQR, interquartile range; KDIGO, Kidney Disease: Improving Global Outcomes; MLR, monocyte-to-lymphocyte ratio; NLR, neutrophil-to-lymphocyte ratio; NPR, neutrophil-to-platelet ratio; $PaCO_2$, arterial partial pressure of carbon dioxide; PaO_2, arterial partial pressure of oxygen; P/F, PaO_2/FiO_2 ratio; PLR, platelet-to-lymphocyte ratio; RPS, ranked probability score; SHAP, Shapley additive explanations; SII, systemic immune-inflammation index; SIRI, systemic inflammation response index.

ALB, albumin; CREA, creatinine; CysC, cystatin C; GLU, glucose; MAE, mean absolute error; MYO, myoglobin; NYHA, New York Heart Association; ROC, receiver operating characteristic; RRT, renal replacement therapy; SD, standard deviation; FiO_2, fraction of inspired oxygen.

Glossary

Ordinal outcome: categories ordered by increasing respiratory–renal support.

Proportional-odds model: regression with shared coefficients across cumulative thresholds.

Out-of-fold prediction: prediction from training data excluding the predicted patient.

Ranked probability score: error in predicted cumulative probabilities; lower is better.

Declarations

Ethics approval and consent to participate

The study was conducted in accordance with the Declaration of Helsinki and its subsequent amendments. The parent cohort and secondary use of its data were approved by the Ethics Committee of Beijing Anzhen Hospital (approval No. KS2024036; April 17, 2024). Written informed consent was obtained from all participants at enrollment. The present analysis was separately approved by the same committee (approval No. 2026311x; September 7, 2026), which waived the requirement for additional informed consent.

Consent for publication

Not applicable.

Availability of data and materials

The clinical data are not publicly available because of ethical and privacy restrictions. De-identified data necessary to reproduce the analyses and the analysis code may be made available from the corresponding author on reasonable request, subject to institutional and ethics-committee approval. The research-use calculator is included in Additional file 2.

Competing interests

The authors declare that they have no competing interests.

Funding

This work was supported by the Capital's Health Development Research Special Fund (No. 2024-2-1053), the Noncommunicable Chronic Diseases-National Science and Technology Major Project (No. 2023ZD0504400), and the Beijing Natural Science Foundation-Capital Clinical Medicine Innovation Joint Fund (No. L2510015). The funders had no role in the study design, data collection, data analysis, data interpretation, manuscript preparation, or decision to submit the work for publication.

Authors' contributions

XS contributed to conceptualization, methodology, investigation, data curation, and formal analysis, and drafted the manuscript. RL, JW and JM contributed to conceptualization, methodology, investigation, data curation, and formal analysis, and critically revised the manuscript. PY contributed to conceptualization, methodology, investigation, and data curation, and critically revised the manuscript. TY, NL and JMa contributed to investigation and data curation, and critically revised the manuscript. BZ, BC and CL performed formal analysis and critically revised the manuscript. YG contributed to conceptualization, methodology, formal analysis, supervision, and funding acquisition, and critically revised the manuscript. JZ contributed to conceptualization, methodology, investigation, data curation, formal analysis, and supervision, and critically revised the manuscript. All authors approved the submitted version and agree to be accountable for their own contributions and for ensuring that questions related to the accuracy or integrity of any part of the work are appropriately investigated and resolved.

Acknowledgements

Not applicable.

Additional files

Additional file 1

File name: Additional_file_1_Supplementary_Material.docx. File format: DOCX. Title: Supplementary methods, figures, and tables. Description: Supplementary Methods S1–S8, Figures S1–S10, and Tables S1–S11.

Additional file 2

File name: Additional_file_2_ATAAD_AKI_Risk_Calculator.zip. File format: ZIP containing HTML and TXT. Title: Offline seven-predictor ATAAD AKI research-use calculator. Description: A locally running calculator of grade-specific probabilities and the expected ordinal score, with

instructions. Extract the ZIP and open the HTML in a modern web browser; no internet connection or server is required. Model version: ATAAD-AKI-ordinal-2026.08.30-reduced7.

References

1. Ko T, Higashitani M, Sato A, Uemura Y, Norimatsu T, Mahara K, et al. Impact of Acute Kidney Injury on Early to Long-Term Outcomes in Patients Who Underwent Surgery for Type A Acute Aortic Dissection. Am J Cardiol. 2015;116:463-8. https://doi.org/10.1016/j.amjcard.2015.04.043.

2. Arnaoutakis GJ, Ogami T, Patel HJ, Pai CW, Woznicki EM, Brinster DR, et al. Acute Kidney Injury in Patients Undergoing Surgery for Type A Acute Aortic Dissection. Ann Thorac Surg. 2023;115:879-85. https://doi.org/10.1016/j.athoracsur.2022.10.037.

3. Roh GU, Lee JW, Nam SB, Lee J, Choi JR, Shim YH. Incidence and Risk Factors of Acute Kidney Injury After Thoracic Aortic Surgery for Acute Dissection. Ann Thorac Surg. 2012;94:766-71. https://doi.org/10.1016/j.athoracsur.2012.04.057.

4. Wang Y, Bellomo R. Cardiac surgery-associated acute kidney injury: risk factors, pathophysiology and treatment. Nat Rev Nephrol. 2017;13:697-711. https://doi.org/10.1038/nrneph.2017.119.

5. Chen Z, Lu X, Liu M, Yu Y, Yu L, Cheng S, et al. Artificial Intelligence–Driven Prediction of Acute Kidney Injury Following Acute Type A Aortic Dissection Surgery in a Chinese Population. J Cardiothorac Vasc Anesth. 2025;39:2729-38. https://doi.org/10.1053/j.jvca.2025.05.047.

6. Cui Y, Chen H, Zhang C, Li B, Li Z. Risk Factors for Stage 3 Acute Kidney Injury after Acute Stanford Type A Aortic Dissection Repair. Thorac Cardiovasc Surg. 2026. https://doi.org/10.1055/a-2923-5881.

7. Luo CC, Zhong YL, Qiao ZY, Li CN, Liu YM, Zheng J, et al. Development and validation of a nomogram for postoperative severe acute kidney injury in acute type A aortic dissection. J Geriatr Cardiol. 2022;19:734-42. https://doi.org/10.11909/j.issn.1671-5411.2022.10.003.

8. Tang Z, Hao H, Tang F, Mao Y, Chen M. Association of systemic inflammation response index with postoperative clinical outcomes among operated patients with aortic dissection: a systematic review with meta-analysis. J Thorac Dis. 2026;18:472. https://doi.org/10.21037/jtd-2026-1-0423.

9. Xu Y, Huang C, Wang Y, Huang C, Xie Y, Liang G, et al. Machine learning prediction of postoperative acute kidney injury in aortic dissection patients using dynamic inflammatory markers and clinical features. BMC Med Inform Decis Mak. 2026;26:153. https://doi.org/10.1186/s12911-026-03443-y.

10. Liu Z, Shen Y, Zou J, Huang W. Preoperative systemic immune-inflammation index as an incremental predictor of postoperative refractory hypoxemia in acute type a aortic dissection. J Cardiothorac Surg. 2026;21:637. https://doi.org/10.1186/s13019-026-04435-9.

11. Urbanowicz T, Olasińska-Wiśniewska A, Michalak M, Rodzki M, Witkowska A, Straburzyńska-Migaj E, et al. The Prognostic Significance of Neutrophil to Lymphocyte Ratio (NLR), Monocyte to Lymphocyte Ratio (MLR) and Platelet to Lymphocyte Ratio (PLR) on Long-Term Survival in Off-Pump Coronary Artery Bypass Grafting (OPCAB) Procedures. Biology (Basel). 2022;11:34. https://doi.org/10.3390/biology11010034.

12. Wang X, Xu H, Tu G, Lai H, Xu J, Li X, et al. A higher preoperative total protein to albumin ratio independently predicted more severe postoperative acute kidney injury in patients with acute type A aortic dissection: a retrospective cohort study of 224 cases. Front Cardiovasc Med. 2025;12:1562388. https://doi.org/10.3389/fcvm.2025.1562388.

13. Xu S, Wu Z, Liu Y, Zhu J, Gong M, Sun L, et al. Influence of Preoperative Serum Albumin on Acute Kidney Injury after Aortic Surgery for Acute Type A Aortic Dissection: A Retrospective Cohort Study. J Clin Med. 2023;12:1581. https://doi.org/10.3390/jcm12041581.

14. Hong Y, Zhang BW, Shi J, Min RX, Wang DY, Kan JX, et al. Impact of admission-blood-glucose-to-albumin ratio on all-cause mortality and renal prognosis in critical patients with coronary artery disease: insights from the MIMIC-IV database. J Geriatr Cardiol. 2025;22:563-77. https://doi.org/10.26599/1671-5411.2025.06.001.

15. Kellum JA, Lameire N, KDIGO AKI Guideline Work Group. Diagnosis, evaluation, and management of acute kidney injury: a KDIGO summary (Part 1). Crit Care. 2013;17:204. https://doi.org/10.1186/cc11454.

16. Collins GS, Moons KGM, Dhiman P, Riley RD, Beam AL, Van Calster B, et al. TRIPOD+AI statement: updated guidance for reporting clinical prediction models that use regression or machine learning methods. BMJ. 2024;385:e078378. https://doi.org/10.1136/bmj-2023-078378.

17. Kursa MB, Rudnicki WR. Feature Selection with the Boruta Package. J Stat Softw. 2010;36:1-13. https://doi.org/10.18637/jss.v036.i11.

18. Lundberg SM, Lee SI. A unified approach to interpreting model predictions. Adv Neural Inf Process Syst. 2017;30:4765-74. https://proceedings.neurips.cc/paper_files/paper/2017/hash/8a20a8621978632d76c43dfd28b67767-Abstract.html. Accessed 7 October 2026.

19. Edlinger M, van Smeden M, Alber HF, Wanitschek M, Van Calster B. Risk prediction models for discrete ordinal outcomes: Calibration and the impact of the proportional odds assumption. Stat Med. 2022;41:1334-60. https://doi.org/10.1002/sim.9281.

20. Vickers AJ, Elkin EB. Decision Curve Analysis: A Novel Method for Evaluating Prediction Models. Med Decis Making. 2006;26:565-74. https://doi.org/10.1177/0272989X06295361.

21. Komaru Y, Bai YZ, Kreisel D, Herrlich A. Interorgan communication networks in the kidney–lung axis. Nat Rev Nephrol. 2024;20:120-36. https://doi.org/10.1038/s41581-023-00760-7.

22. Yang C, Hou P, Wang D, Wang Z, Duan W, Liu J, et al. Serum Myoglobin Is Associated With Postoperative Acute Kidney Injury in Stanford Type A Aortic Dissection. Front Med (Lausanne). 2022;9:821418. https://doi.org/10.3389/fmed.2022.821418.

23. Dai A, Zhou Z, Jiang F, Guo Y, Asante DO, Feng Y, et al. Incorporating intraoperative blood pressure time-series variables to assist in prediction of acute kidney injury after type a acute aortic dissection repair: an interpretable machine learning model. Ann Med. 2023;55:2266458. https://doi.org/10.1080/07853890.2023.2266458.

24. Herro R, Grimes HL. The diverse roles of neutrophils from protection to pathogenesis. Nat Immunol. 2024;25:2209-19. https://doi.org/10.1038/s41590-024-02006-5.

25. Brown N, Sullo N, Tyson N, Eagle–Hemming B, Lai FY, Sheikh S, et al. Acute kidney injury after cardiac surgery is associated with platelet activation. J Thromb Haemost. 2025;23:2776-89. https://doi.org/10.1016/j.jtha.2025.06.009.

26. Li S, Nordick KV, Murrieta-Álvarez I, Kirby RP, Bhattacharya R, Garcia I, et al. Prolonged Cardiopulmonary Bypass Time-Induced Endothelial Dysfunction via Glypican-1 Shedding, Inflammation, and Matrix Metalloproteinase 9 in Patients Undergoing Cardiac Surgery. Biomedicines. 2025;13:33. https://doi.org/10.3390/biomedicines13010033.

27. Wollborn J, Zhang Z, Gaa J, Gentner M, Hausmann C, Saenger F, et al. Angiopoietin-2 is associated with capillary leak and predicts complications after cardiac surgery. Ann Intensive Care. 2023;13:70. https://doi.org/10.1186/s13613-023-01165-2.

28. Yuanxi L, Li Z, Jiang X, Jiang Y, Wang D, Xue Y. A novel nomogram for predicting prolonged mechanical ventilation after acute type A aortic dissection surgery: a retrospective study investigating the impact of ventilation duration on postoperative outcomes. Ann Med. 2024;56:2392871. https://doi.org/10.1080/07853890.2024.2392871.

29. Diaz-Castrillon CE, Brown JA, Navid F, Serna-Gallegos D, Yousef S, Thoma F, et al. The impact of prolonged mechanical ventilation after acute type A aortic dissection repair. J Thorac Cardiovasc Surg. 2024;167:1672-1679.e2. https://doi.org/10.1016/j.jtcvs.2022.07.007.

Figure legends

Figure 1. Study design, outcome hierarchy, and ordinal separation.

(A) Patient flow: 1186 parent-cohort patients; 579 without postoperative AKI; 607 with postoperative AKI; six mutually exclusive pre-index exclusions (CRRT, n = 3; reintubation, n = 2; death, n = 1); final cohort, n = 601. (B) The first postoperative fulfillment of KDIGO AKI criteria defined the index; all predictors preceded it. (C) Grade 0, neither respiratory failure nor CRRT (n = 285); Grade 1, respiratory failure without CRRT (n = 170); Grade 2, CRRT irrespective of respiratory status (n = 146). (D) Out-of-fold expected score by grade.

Abbreviations: AKI, acute kidney injury; ATAAD, acute type A aortic dissection; CPB, cardiopulmonary bypass; CRRT, continuous renal replacement therapy; KDIGO, Kidney Disease: Improving Global Outcomes.

Figure 2. Predictor associations, marginal effects, and selection stability.

(A) Selection-conditioned common odds ratios per 1-SD increase from the proportional-odds ordinal logistic model; points indicate odds ratios and horizontal lines 95% confidence intervals. (B) Average marginal prediction curves for representative predictors, calculated on a 251-point empirical percentile grid from the 5th to the 95th percentile while retaining each patient's observed values for all other predictors and averaging the patient-level expected ordinal scores. (C) Predictor-selection frequency across the 50 outer training folds; the dashed line denotes an 80% selection frequency.

Abbreviations: AISI, aggregate index of systemic inflammation; ALB, albumin; CPB, cardiopulmonary bypass; CREA, creatinine; CysC, cystatin C; eGFR, estimated glomerular filtration rate; GAR, glucose-to-albumin ratio; MYO, myoglobin; NPR, neutrophil-to-platelet ratio; PLR, platelet-to-lymphocyte ratio; PLT, platelet count; SD, standard deviation; SII, systemic immune-inflammation index.

Figure 3. Internal validation of the primary ordinal model.

(A) Cumulative ROC curves for Grade ≥1 and Grade 2 from averaged out-of-fold predictions. (B) Observed versus predicted event proportions by probability decile. (C) Decision curves versus treat-all and treat-none strategies over the displayed thresholds.

Abbreviation: ROC, receiver operating characteristic.

Figure 4. Incremental and ablation analyses of selected predictor domains.

Change in ranked probability score (ΔRPS) relative to the corresponding reduced model; negative values favor inclusion of the evaluated predictors. (A) GAR and its glucose and albumin components. (B) inflammatory information represented by raw blood-cell counts, composite inflammatory indices, their combination, or the selected full inflammatory feature set. (C) forced inclusion of direct respiratory measures. Points indicate paired differences in RPS and horizontal lines 95% confidence intervals; the vertical dashed line indicates no difference.

Abbreviations: A–aDO_2, alveolar–arterial oxygen gradient; ALB, albumin; GAR, glucose-to-albumin ratio; GLU, glucose; $PaCO_2$, arterial partial pressure of carbon dioxide; PaO_2, arterial partial pressure of oxygen; P/F, PaO_2/FiO_2 ratio; RPS, ranked probability score.

Tables

Table 1. Selected baseline and perioperative characteristics across the ordered outcome grades

Characteristic	Overall (n = 601)	Grade 0 (n = 285)	Grade 1 (n = 170)	Grade 2 (n = 146)	P value
Preoperative demographics and medical history					
Female sex, n (%)	152 (25.29%)	68 (23.86%)	38 (22.35%)	46 (31.51%)	0.131
Age, years, median [IQR]	53 [43, 60]	51 [42, 58]	54 [42, 60]	56 [44, 60]	0.020
Body mass index, kg/m², median [IQR]	26.7 [24.5, 29.7]	26.8 [24.7, 30.2]	26.8 [24.9, 29.9]	26.1 [23.5, 29.4]	0.033
Hypertension, n (%)	505 (84.03%)	239 (83.86%)	153 (90.00%)	113 (77.40%)	0.010
Cerebrovascular disease, n (%)	91 (15.14%)	27 (9.47%)	30 (17.65%)	34 (23.29%)	<0.001
Valvular heart disease, n (%)	268 (44.59%)	119 (41.75%)	80 (47.06%)	69 (47.26%)	0.413
Coronary artery disease, n (%)	103 (17.14%)	37 (12.98%)	33 (19.41%)	33 (22.60%)	0.028
Chronic respiratory disease (any non-zero code), n (%)	6 (1.00%)	2 (0.70%)	2 (1.18%)	2 (1.37%)	0.766
Diabetes mellitus, n (%)	38 (6.32%)	18 (6.32%)	14 (8.24%)	6 (4.11%)	0.323
Previous cardiac surgery, n (%)	18 (3.00%)	6 (2.11%)	6 (3.53%)	6 (4.11%)	0.457
Preoperative laboratory measurements					

Characteristic	Overall (n = 601)	Grade 0 (n = 285)	Grade 1 (n = 170)	Grade 2 (n = 146)	P value
Preoperative C-reactive protein, mg/L, median [IQR]	6.85 [2.45, 29.63]	7.27 [2.73, 29.80]	6.22 [2.53, 25.71]	6.46 [1.92, 30.98]	0.748
Preoperative alanine aminotransferase, U/L, median [IQR]	21.2 [15.0, 34.0]	22.0 [15.0, 34.0]	21.0 [15.0, 31.0]	22.0 [15.0, 35.8]	0.788
Preoperative aspartate aminotransferase, U/L, median [IQR]	22.0 [17.0, 30.0]	21.0 [17.0, 30.0]	21.0 [17.0, 29.0]	25.0 [19.1, 33.8]	0.010
Preoperative albumin, g/L, median [IQR]	39.9 [37.2, 42.3]	40.4 [38.1, 43.0]	39.5 [37.4, 42.2]	38.8 [36.0, 41.6]	<0.001
Preoperative urea, mmol/L, median [IQR]	6.31 [5.38, 7.68]	6.19 [5.27, 7.36]	6.37 [5.49, 8.14]	6.60 [5.50, 8.05]	0.117
Preoperative creatinine, μmol/L, median [IQR]	80.1 [66.1, 101.9]	77.1 [63.1, 96.7]	82.7 [68.2, 99.0]	87.0 [69.7, 118.5]	0.001
Preoperative cystatin C, mg/L, median [IQR]	1.05 [0.83, 1.34]	0.96 [0.79, 1.24]	1.11 [0.88, 1.37]	1.15 [0.92, 1.70]	<0.001
Preoperative lactate dehydrogenase, U/L, median [IQR]	212.0 [184.0, 256.0]	206.0 [179.0, 249.0]	208.5 [185.0, 248.2]	233.0 [194.0, 275.2]	0.001
Preoperative high-sensitivity cardiac troponin I, ng/L, median [IQR]	11.6 [5.1, 45.3]	10.8 [5.1, 38.2]	11.2 [5.1, 31.2]	16.3 [5.3, 66.8]	0.222
Preoperative myoglobin, ng/mL, median [IQR]	59.5 [22.1, 200.0]	34.9 [19.1, 153.8]	67.7 [29.4, 205.0]	134.3 [35.2, 245.9]	<0.001
Preoperative lactate, mmol/L, median [IQR]	1.70 [1.20, 2.50]	1.70 [1.20, 2.30]	1.80 [1.20, 2.55]	1.70 [1.20, 2.90]	0.481
Preoperative neutrophil count, $\times 10^9$/L, median [IQR]	9.33 [6.24, 12.39]	8.68 [6.22, 11.71]	10.05 [7.19, 12.85]	9.52 [5.80, 12.38]	0.056

Characteristic	Overall (n = 601)	Grade 0 (n = 285)	Grade 1 (n = 170)	Grade 2 (n = 146)	P value
Preoperative lymphocyte count, $\times 10^9$/L, median [IQR]	1.12 [0.72, 1.53]	1.10 [0.71, 1.50]	1.10 [0.77, 1.56]	1.16 [0.70, 1.60]	0.728
Preoperative monocyte count, $\times 10^9$/L, median [IQR]	0.580 [0.420, 0.790]	0.580 [0.400, 0.760]	0.615 [0.453, 0.847]	0.530 [0.410, 0.748]	0.056
Preoperative glucose, mmol/L, median [IQR]	7.13 [6.07, 8.34]	6.98 [6.01, 7.98]	7.33 [5.97, 8.38]	7.51 [6.29, 8.77]	0.019
Preoperative glucose-to-albumin ratio, median [IQR]	0.182 [0.153, 0.214]	0.171 [0.151, 0.202]	0.186 [0.151, 0.219]	0.196 [0.166, 0.229]	<0.001
Preoperative derived inflammatory indices					
Preoperative AISI (back-transformed), median [IQR]	946.3 [493.4, 1672.5]	928.5 [493.6, 1484.8]	1040.8 [593.8, 1947.3]	858.2 [345.0, 1634.5]	0.076
Preoperative MLR (back-transformed), median [IQR]	0.552 [0.370, 0.828]	0.529 [0.357, 0.793]	0.619 [0.402, 0.834]	0.541 [0.349, 0.836]	0.206
Preoperative NLR (back-transformed), median [IQR]	9.14 [4.76, 14.28]	8.63 [4.39, 13.64]	10.04 [5.73, 14.24]	9.12 [4.08, 16.40]	0.512
Preoperative NPR (back-transformed), median [IQR]	0.055 [0.033, 0.077]	0.052 [0.030, 0.072]	0.059 [0.039, 0.077]	0.058 [0.032, 0.081]	0.026
Preoperative PLR (back-transformed), median [IQR]	171.0 [120.5, 240.2]	178.6 [122.2, 245.1]	171.0 [123.7, 227.9]	155.7 [109.9, 244.5]	0.257
Preoperative SII (back-transformed), median [IQR]	1601 [872, 2664]	1573 [887, 2497]	1671 [979, 2776]	1467 [735, 2840]	0.534
Preoperative SIRI (back-transformed), median [IQR]	5.27 [2.54, 9.43]	4.89 [2.77, 8.11]	6.37 [3.32, 9.99]	5.65 [1.97, 10.25]	0.040
Preoperative respiratory measurements					
Preoperative $PaCO_2$, mmHg, median [IQR]	35.6 [32.3, 39.1]	35.6 [33.0, 39.1]	36.1 [32.2, 39.2]	35.0 [31.5, 39.1]	0.339
Preoperative PaO_2, mmHg, median [IQR]	95.0 [78.9, 124.0]	96.0 [78.7, 126.8]	91.3 [77.7, 117.5]	99.3 [82.7, 126.5]	0.157

Characteristic	Overall (n = 601)	Grade 0 (n = 285)	Grade 1 (n = 170)	Grade 2 (n = 146)	P value
Preoperative P/F ratio, median [IQR]	447.5 [371.0, 590.5]	457.1 [369.7, 601.5]	432.0 [361.5, 548.5]	478.0 [390.5, 602.5]	0.093
Intraoperative measurements					
Cardiopulmonary bypass time, min, median [IQR]	183.0 [160.0, 219.0]	176.0 [154.5, 203.0]	186.5 [159.8, 215.2]	210.5 [174.5, 260.8]	<0.001
Immediate postoperative cell counts and inflammatory indices					
Immediate postoperative lymphocyte count, $\times 10^9$/L, median [IQR]	0.540 [0.370, 0.800]	0.500 [0.330, 0.688]	0.570 [0.390, 0.880]	0.590 [0.383, 0.895]	0.002
Immediate postoperative neutrophil count, $\times 10^9$/L, median [IQR]	10.3 [7.8, 13.3]	10.2 [7.9, 12.8]	10.6 [7.7, 13.5]	10.0 [7.7, 13.6]	0.773
Immediate postoperative monocyte count, $\times 10^9$/L, median [IQR]	0.500 [0.300, 0.700]	0.500 [0.283, 0.677]	0.510 [0.310, 0.740]	0.510 [0.323, 0.720]	0.357
Immediate postoperative platelet count, $\times 10^9$/L, median [IQR]	84.0 [55.0, 121.0]	100.0 [71.2, 139.8]	86.0 [62.0, 119.0]	53.0 [34.2, 80.0]	<0.001
Immediate postoperative AISI (back-transformed), median [IQR]	767.2 [345.3, 1611.9]	901.8 [457.6, 1902.0]	794.6 [382.4, 1621.6]	417.6 [168.0, 1059.1]	<0.001
Immediate postoperative MLR (back-transformed), median [IQR]	0.900 [0.552, 1.371]	0.928 [0.608, 1.387]	0.934 [0.525, 1.375]	0.826 [0.505, 1.363]	0.193

Characteristic	Overall (n = 601)	Grade 0 (n = 285)	Grade 1 (n = 170)	Grade 2 (n = 146)	P value
Immediate postoperative NLR (back-transformed), median [IQR]	19.0 [12.4, 28.2]	20.5 [13.9, 29.2]	18.7 [11.8, 28.0]	16.6 [10.0, 25.1]	0.005
Immediate postoperative NPR (back-transformed), median [IQR]	0.118 [0.082, 0.178]	0.103 [0.070, 0.144]	0.116 [0.083, 0.168]	0.177 [0.120, 0.304]	<0.001
Immediate postoperative PLR (back-transformed), median [IQR]	160.0 [86.5, 277.6]	205.6 [124.7, 350.0]	146.2 [88.0, 244.2]	97.0 [44.3, 173.8]	<0.001
Immediate postoperative SII (back-transformed), median [IQR]	1579 [782, 2964]	2054 [1139, 3625]	1541 [810, 2632]	881 [388, 1839]	<0.001
Immediate postoperative SIRI (back-transformed), median [IQR]	9.13 [4.87, 16.47]	9.17 [5.07, 16.81]	9.09 [5.22, 16.24]	8.63 [4.03, 15.50]	0.452
Immediate postoperative laboratory and respiratory measurements					
Immediate postoperative creatinine, μmol/L, median [IQR]	139.3 [110.4, 187.2]	127.6 [104.5, 157.4]	138.2 [110.7, 191.9]	181.4 [136.9, 249.1]	<0.001
Immediate postoperative urea, mmol/L, median [IQR]	12.2 [9.4, 16.4]	12.0 [9.0, 15.2]	12.1 [9.2, 16.8]	13.2 [10.2, 17.6]	0.014
Immediate postoperative glucose, mmol/L, median [IQR]	7.83 [6.54, 9.84]	7.42 [6.37, 9.00]	8.04 [6.58, 10.05]	8.38 [6.95, 11.33]	<0.001
Immediate postoperative albumin, g/L, median [IQR]	27.3 [23.6, 30.7]	28.1 [24.7, 31.3]	27.2 [24.1, 30.1]	25.2 [21.0, 29.5]	<0.001

Characteristic	Overall (n = 601)	Grade 0 (n = 285)	Grade 1 (n = 170)	Grade 2 (n = 146)	P value
Immediate postoperative glucose-to-albumin ratio, median [IQR]	0.297 [0.235, 0.383]	0.275 [0.215, 0.346]	0.305 [0.242, 0.375]	0.343 [0.258, 0.483]	<0.001
Immediate postoperative $PaCO_2$, mmHg, median [IQR]	45.0 [40.8, 49.3]	45.5 [41.1, 49.0]	45.5 [41.3, 49.9]	44.0 [39.7, 48.6]	0.346
Immediate postoperative PaO_2, mmHg, median [IQR]	112.0 [81.5, 150.5]	115.5 [83.5, 151.2]	102.5 [78.1, 140.0]	109.0 [78.4, 164.0]	0.036
Immediate postoperative lactate, mmol/L, median [IQR]	2.70 [1.70, 4.80]	2.40 [1.55, 3.65]	2.70 [1.80, 4.50]	3.90 [2.23, 6.80]	<0.001
Immediate postoperative $A–aDO_2$, mmHg, median [IQR]	114.8 [83.3, 155.3]	119.2 [85.1, 155.3]	104.5 [80.8, 149.0]	113.8 [78.5, 167.1]	0.048
Immediate postoperative P/F ratio, median [IQR]	531.0 [386.8, 721.0]	552.0 [396.0, 744.0]	482.0 [370.0, 667.0]	512.0 [373.0, 796.0]	0.023

Data are median [interquartile range] or n (%). P values are descriptive overall comparisons and were not adjusted for multiple comparisons. Cell-count indices are displayed on the original scale and were log-transformed for modeling. Immediate postoperative values were the first measurements within 2 h of surgery. AKI stage used creatinine and urine-output criteria, excluding RRT because CRRT defined Grade 2.

Abbreviations: AISI, aggregate index of systemic inflammation; $A–aDO_2$, alveolar–arterial oxygen gradient; CPB, cardiopulmonary bypass; eGFR, estimated glomerular filtration rate; GAR, glucose-to-albumin ratio; IQR, interquartile range; MLR, monocyte-to-lymphocyte ratio; NLR, neutrophil-to-lymphocyte ratio; NPR, neutrophil-to-platelet ratio; NYHA, New York Heart Association; $PaCO_2$, arterial partial pressure of carbon dioxide; PaO_2,

503 arterial partial pressure of oxygen; P/F, PaO_2/FiO_2 ratio; PLR, platelet-to-lymphocyte ratio; SII, systemic immune-inflammation index; SIRI, systemic

504 inflammation response index.

505 For SI conversion, multiply pressures in mmHg by 0.133322 to obtain kPa; 1 ng/mL equals 1 μg/L.

506 **Table 2. Clinical phenotypes across the ordered outcome grades and Grade 2 subtypes**

Outcome group	No. of patients	Mechanical ventilation, median (IQR), h	ICU stay, median (IQR), h	Hospital stay, median (IQR), d	In-hospital mortality, No. (%)
Grade 0	285	17.0 [13.0, 30.0]	57.0 [35.0, 83.0]	14 [10, 18]	3 (1.1%)
Grade 1	170	116.5 [73.2, 198.8]	192.0 [130.3, 288.0]	17 [13, 23]	18 (10.6%)
Grade 2	146	119.5 [58.5, 233.5]	204.0 [79.0, 318.0]	15 [9, 25]	37 (25.3%)
Grade 2a	37	30.0 [16.0, 44.0]	59.0 [35.0, 168.0]	13 [3, 22]	9 (24.3%)
Grade 2b	109	158.0 [89.0, 270.0]	240.0 [167.3, 354.5]	16 [10, 26]	28 (25.7%)

507 Data are presented as median [interquartile range] or n (%). Grade 0 denotes neither respiratory failure nor CRRT after the index time; Grade 1 denotes

508 respiratory failure without subsequent CRRT; and Grade 2 denotes CRRT irrespective of respiratory-failure status. Grade 2a denotes CRRT without

509 respiratory failure and Grade 2b CRRT with respiratory failure. Respiratory failure was defined as invasive mechanical ventilation >48 h, with the

510 threshold first crossed after the index time, or reintubation after the index time. Mortality was not incorporated into the outcome grading. Mechanical-

511 ventilation duration is reported descriptively because it contributes to the respiratory-failure definition.

Abbreviations: CRRT, continuous renal replacement therapy; ICU, intensive care unit; IQR, interquartile range.

Table 3. Internal validation performance of the four ordinal prediction models

Model	RPS	Normalized multiclass Brier score	Ordinal C-index	AUC, Grade ≥1	AUC, Grade 2	MAE	Weighted κ
Ordered logistic regression	0.1705	0.1794	0.7632	0.7476	0.8299	0.5829	0.4458
Ordered random forest	0.1759	0.1854	0.7513	0.7318	0.8123	0.5994	0.4155
Ordered XGBoost	0.1776	0.1872	0.7486	0.7249	0.8104	0.5859	0.4152
Ordered LightGBM	0.1867	0.1957	0.7397	0.7155	0.8008	0.5839	0.4219

Estimates use averaged out-of-fold predictions. Higher is better for ordinal C-index, AUC, and weighted κ; lower is better for RPS, normalized Brier score, and MAE. Confidence intervals and paired comparisons appear in the Supplementary Material.

Abbreviations: AUC, area under the receiver operating characteristic curve; MAE, mean absolute error; RPS, ranked probability score.

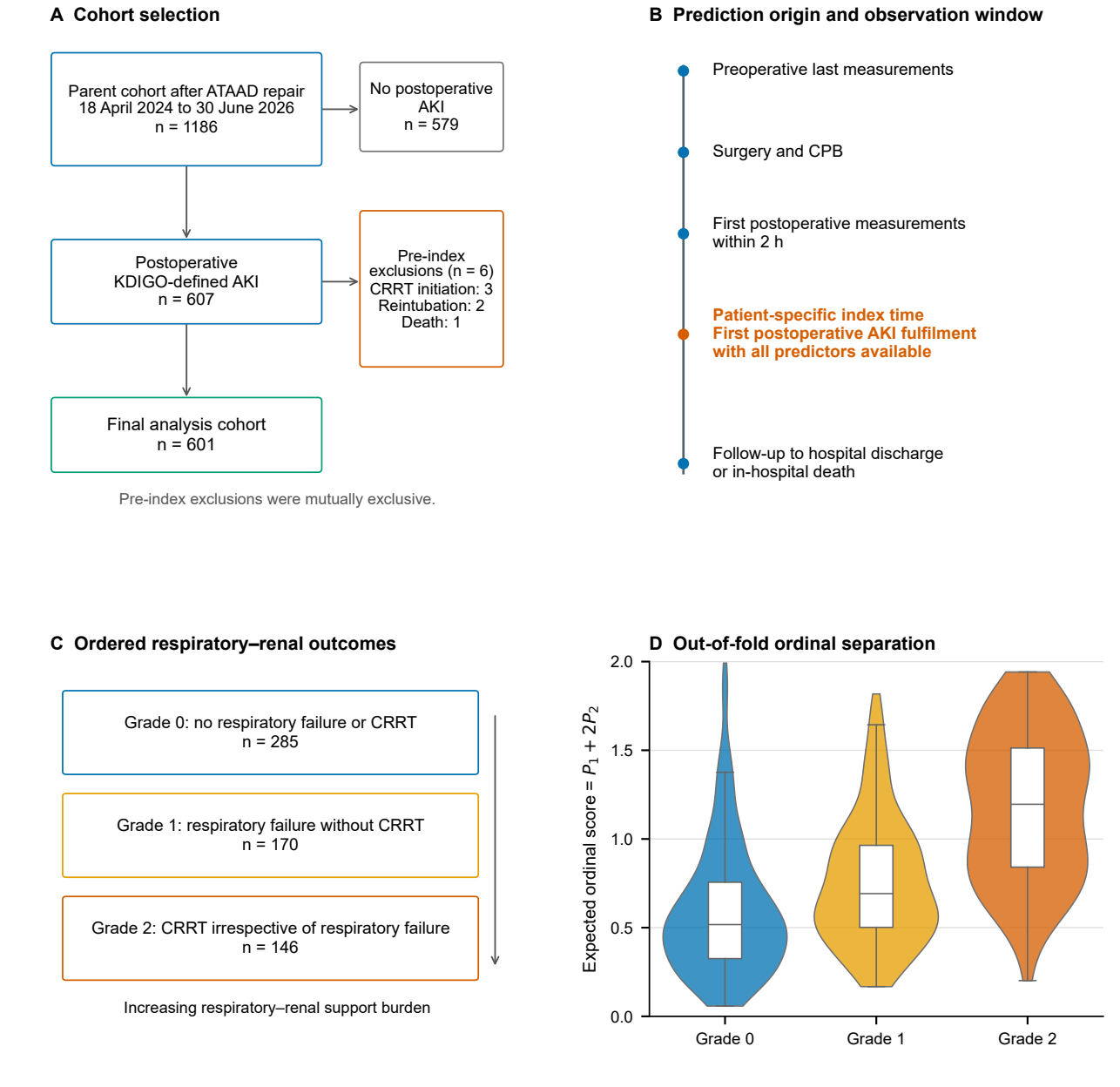
A Cohort selection
Parent cohort after ATAAD repair
18 April 2024 to 30 June 2026
n = 1186
No postoperative AKI
n = 579
Postoperative KDIGO-defined AKI
n = 607
Pre-index exclusions (n = 6)
CRRT initiation: 3
Reintubation: 2
Death: 1
Final analysis cohort
n = 601
Pre-index exclusions were mutually exclusive.
B Prediction origin and observation window
Preoperative last measurements
Surgery and CPB
First postoperative measurements within 2 h
Patient-specific index time
First postoperative AKI fulfilment with all predictors available
Follow-up to hospital discharge or in-hospital death
C Ordered respiratory–renal outcomes
Grade 0: no respiratory failure or CRRT
n = 285
Grade 1: respiratory failure without CRRT
n = 170
Grade 2: CRRT irrespective of respiratory failure
n = 146
Increasing respiratory–renal support burden
D Out-of-fold ordinal separation
Expected ordinal score = $P_1 + 2P_2$
2.0
1.5
1.0
0.5
0.0
Grade 0
Grade 1
Grade 2

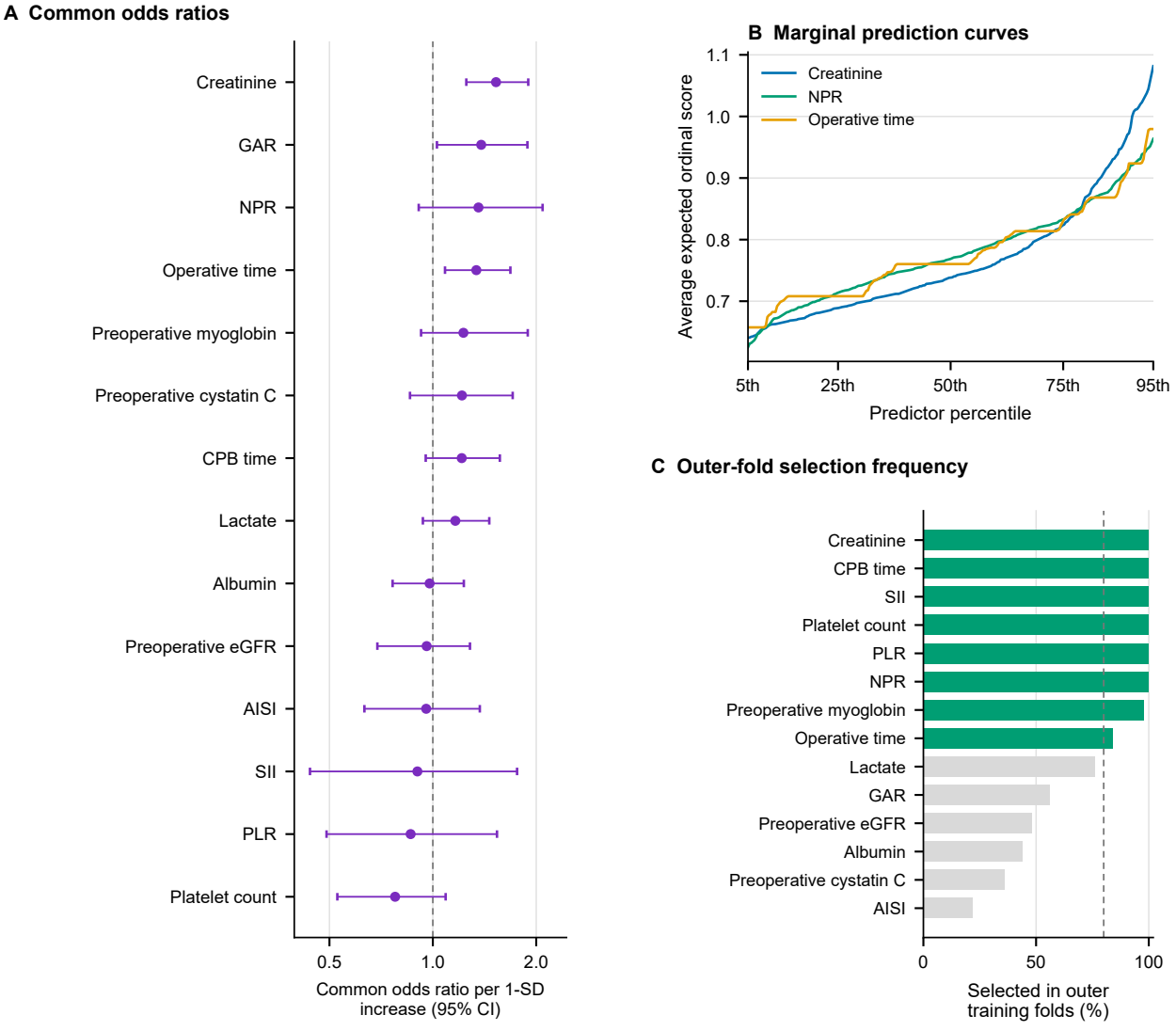
A Common odds ratios
Creatinine
GAR
NPR
Operative time
Preoperative myoglobin
Preoperative cystatin C
CPB time
Lactate
Albumin
Preoperative eGFR
AISI
SII
PLR
Platelet count
0.5
1.0
2.0
Common odds ratio per 1-SD increase (95% CI)
B Marginal prediction curves
Creatinine
NPR
Operative time
Average expected ordinal score
1.1
1.0
0.9
0.8
0.7
5th
25th
50th
75th
95th
Predictor percentile
C Outer-fold selection frequency
Creatinine
CPB time
SII
Platelet count
PLR
NPR
Preoperative myoglobin
Operative time
Lactate
GAR
Preoperative eGFR
Albumin
Preoperative cystatin C
AISI
0
50
100
Selected in outer training folds (%)

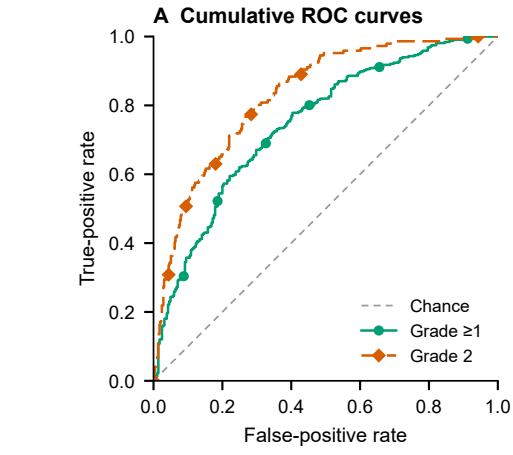

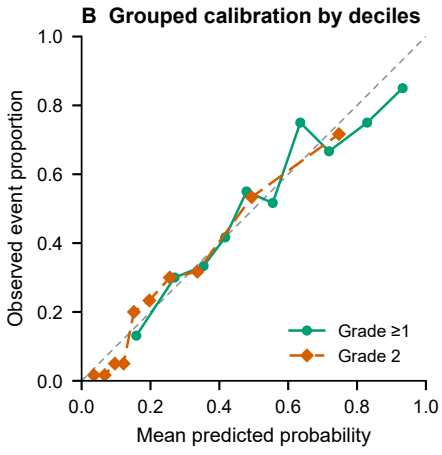

C Decision curves

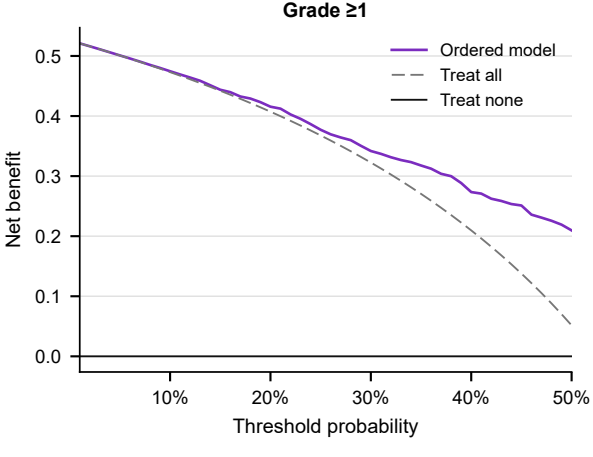

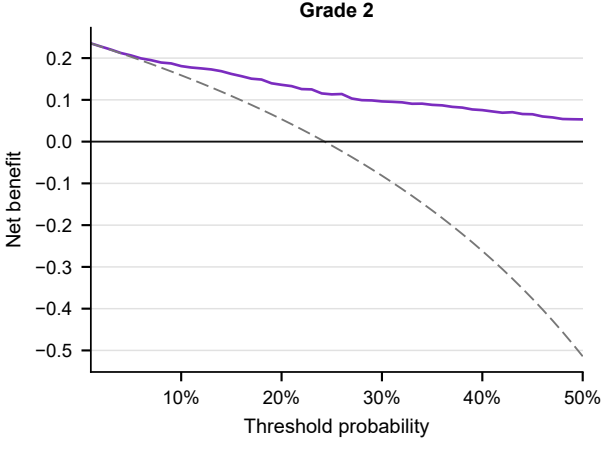

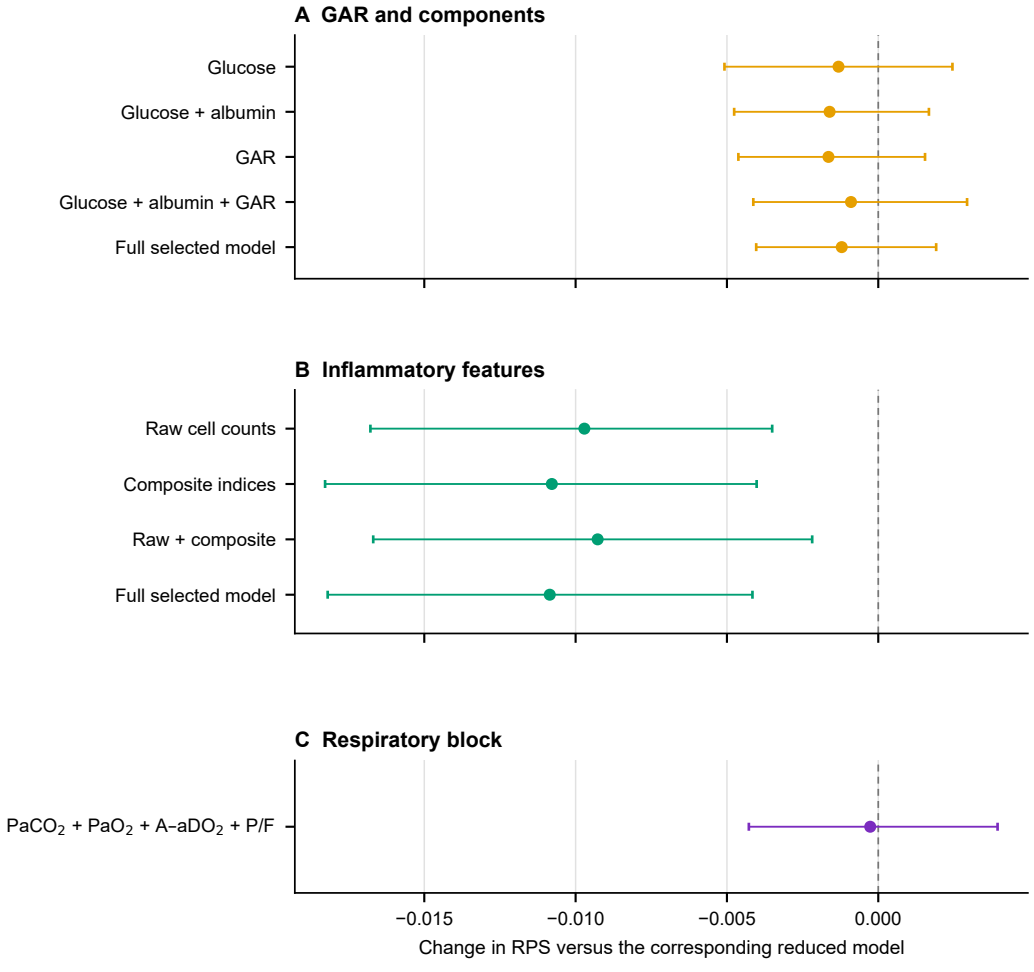
A GAR and components
Glucose
Glucose + albumin
GAR
Glucose + albumin + GAR
Full selected model
B Inflammatory features
Raw cell counts
Composite indices
Raw + composite
Full selected model
C Respiratory block
PaCO2 + PaO2 + A–aDO2 + P/F
−0.015
−0.010
−0.005
0.000
Change in RPS versus the corresponding reduced model

Supplementary Files

This is a list of supplementary files associated with this preprint. Click to download.

- Additionalfile1SupplementaryMaterial.docx
- Additionalfile2ATAADAKIRiskCalculator.zip